.

Citation: *Egypt.Acad.J.Biolog.Sci. (C.Physiology and Molecular biology) Vol. 16(2) pp351-364 (2024)*
DOI: 10.21608/EAJBSC.2024.394788

Egypt. Acad. J. Biolog. Sci., 16(2):351-364 (2024)

Egyptian Academic Journal of Biological Sciences
C. Physiology & Molecular Biology
ISSN 2090-0767
www.eajbsc.journals.ekb.eg

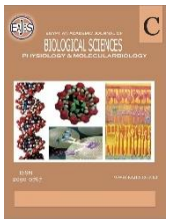

Exploring Bacterial Interactions with Microplastics in the Human Gut Microbiome

Alqurashi, Abdulmajeed[1] ; El-Naggar, Sabry[2] and Soliman, Ahmed[3]
[1]Department of Biology, College of Science, Taibah University, Medinah 42353, Saudi Arabia.
[2]Zoology Department, Faculty of Science, Tanta University, Tanta, Egypt.
[3]Biotechnology Program, Faculty of Agriculture, Ain Shams University, Cairo, Egypt.
***E-mail:** aqurashi@taibahu.edu.sa

ARTICLE INFO
Article History
Received:31/10/2024
Accepted:3/12/2024
Available:7/12/2024

Keywords:
Microplastics, Gut microbiome, Molecular docking, DNA gyrase B, ADMET analysis.

ABSTRACT

Microplastics (MPs) have potential effects on human health due to their existence in the environment. Because of their small size, these MPs can be consumed by a wide range of living things, which might cause inflammatory reactions and possibly have serious negative effects on important organs. Although the ecotoxicological effects of MPs have been the subject of numerous studies, little is known about how they interact with bacteria, particularly those found in the human gut microbiome. The presence of MPs may disturb the gut microbiome, which is important for the immune system and digestive processes. With an emphasis on the binding processes and possible health impacts, this study investigates the interactions between MPs and bacteria in the human gut microbiome concentrating on the binding processes and any health impacts. To evaluate binding interactions with MPs of different sizes, the amino acid sequences of DNA gyrase B from *Fusobacterium nucleatum*, *Dorea longicatena*, and *Coprococcus sp*. were extracted and prepared for docking simulations. Using AutoDock Vina, molecular docking simulations were run. To find possible interaction locations, the top-scoring binding modes were examined. The behavior of these MPs particles within the human body, including their absorption, distribution, metabolism, excretion, and toxicity, was also predicted using the ADMET-lab 2.0 software. This work gave basic knowledge of the interactions between bacteria and MPs in the human gut and shed light on possible health hazards related to MP exposure.

INTRODUCTION

Due to the widespread dispersion of microplastics (MPs) in the environment, there is a notable variation in concentration across different ecosystems. By 2050, it's predicted that there will be more plastic waste in the ocean than fish, because of the widespread use of various types of plastic (Awuchi and Awuchi 2019). Plastic decomposes into ever-tinier particles with time and is an extremely durable substance with a lengthy half-life (Anwaruzzaman *et al.,* 2022). These minuscule particles are referred to as MPs. MPs continue to break down and become small enough for a variety of species to consume (Bajt, 2021). Numerous organisms have demonstrated inflammatory responses to MPs that are comparable to those triggered by bacteria, suggesting that MPs may serve as a conduit for the transfer of pathogens to these organisms (Pirsaheb *et al*., 2020; Tabl *et al.,* 2023). Our knowledge of MPs' effects on these organisms is currently lacking. A growing body of ecotoxicological research has been done to determine how MPs affect human health.

On the other hand, not many studies have been done on the relationships that MPs have with bacteria or how they affect related hosts. Since microorganisms are the basis of many food webs and are essential to the general health of living things, it is crucial to comprehend these interactions. Therefore, any detrimental impacts that MPs may have on microbes may also affect higher-order creatures and ecosystems as a whole (Bhattacharya and Khare, 2022). The precise processes by which bacteria in the gut attach to MPs are not well documented in the literature at this time. Furthermore, nothing is known about the possible health consequences of MPs on the human gut flora. Given the enormous species diversity and density of the gut microbiome—which is thought to support trillions of bacteria from hundreds of species—this information gap is crucial (Moeller and Sanders 2020). Irritable bowel syndrome, inflammatory bowel disease, and even some neurodegenerative illnesses have all been connected to disruptions in the gut microbiota (Gomaa, 2020).

There is an urgent need to have a fuller understanding of the interactions between MPs and the gut and the potential health repercussions. To fully understand the processes of bacterial binding, possible alteration of the microbiome, and the leakage of toxic chemicals from MPs into the gut environment, more research is necessary. This information is crucial for developing mitigation techniques for human exposure to MPs and safeguarding the delicate balance of the gut microbiota. This study is important because it explores the relationship between gut flora, health, and plastic pollution. The field of bacteria-MP interactions and their impact on human health is a fascinating and developing one, and our study will lay the groundwork for it.

MATERIALS AND METHODS

Protein Retrieval and Preparation:

To obtain the 3D structures, the amino acid sequences of DNA gyrase B from three distinct species were obtained from the UniProt database: *Fusobacterium nucleatum*, (UniProt ID: Q7P5Y7), *Dorea longicatena* (UniProt ID: A0A3E5GB93), and *Coprococcus sp*. (UniProt ID: A0A3A6JBC1). When it came time to dock the modeled structures, AutoDock Tools 1.5.7 was used (Morris *et al.,* 2009). This procedure included giving the protein structures Gasteiger charges, combining non-polar hydrogens, and adding polar hydrogens.

Binding Site Prediction:

The CB-Dock 2 online service was utilized to identify the possible binding sites on the protein structures that were created (Liu *et al.,* 2022). Combining the output of multiple binding site prediction algorithms currently in use, CB-Dock 2 predicts binding sites using a consensus-based method.

Ligand Preparation:

Three different ligands were employed to mimic the possible binding of MP particles of varied sizes. The ligands were reduced using the MMFF94 force field in Avogadro 1.2.0 and drawn using the free online version of Marvin JS (Cherinka *et al.*, 2019). Next, using AutoDock Tools 1.5.7 (Morris *et al.,* 2009), the reduced ligand structures were translated to PDBQT format.

Molecular Docking:

Three distinct ligands were used to simulate the probable binding of MP particles of varying sizes. Avogadro 1.2.0 (Hanwell *et al.*, 2012), MMFF94 force field was used to minimize the ligands, and Marvin JS (Cherinka *et al.*, 2019), a free online tool, was used to draw them. After that, the reduced ligand structures were converted to PDBQT format using AutoDock Tools 1.5.7 (Morris *et al.,* 2009).

ADMET Calculation:

The program used for ADMET (Absorption, distribution, metabolism, excretion, and toxicity) calculations was ADMET-lab 2.0 (Xiong *et al.,* 2021). This required entering a compound's SMILES code into ADMET-lab for analysis, a program that makes predictions about a compound's potential physiological responses.

RESULTS

The binding affinities (ΔG) of several MP substances with DNA gyrase B from three distinct organisms *F. nucleatum, D. longicatena,* and *Coprococcus* sp. were displayed in Table 1. There was a stronger binding affinity between the MPs and the enzyme, the lower (more negative) the ΔG value. Among the three species, polycarbonate3 had the highest binding affinity, with ΔG values ranging from -3.9 to -10.2 kcal/mol. In all three organisms, polyethylene1, polyethylene2, and polyethylene3 consistently exhibit the lowest binding affinities; indicating a subpar interaction with DNA gyrase B. Diverse organisms exhibit varying binding affinities for the same MPs molecule, suggesting the possibility of species-specific interactions.

Among the tested MPs, polycarbonate3 exhibits the highest binding affinity for all three organisms; *F. nucleatum, D. longicatena,* and *Coprococcus* sp. had ΔG values of -8.8, -3.9, and -10.2 kcal/mol, respectively. Conversely, polyethylene1, polyethylene2, and polyethylene3 consistently exhibit the lowest binding affinities (ΔG values ranging from -2.7 to -4.1 kcal/mol) among all three organisms.

The DNA gyrase B enzyme from *F. nucleatum* and polyethylene terephthalate3 interacted with a comparatively high binding affinity of -7.4 kcal/mol. Several typical hydrogen bonds are formed by polyethylene terephthalate3 with residues such as ASN47, TYR87, GLY103, ASN109, and GLY120 (Fig. 1). The DNA gyrase B enzyme from *D. longicatena* and polycarbonate1 (PC1) showed a comparatively high binding affinity of -7.1 kcal/mol in their interactions. Through polar interactions, PC1 creates a typical hydrogen bond with the ARG396 residue, which may help stabilize the MPs-enzyme complex (Fig. 2).

Table 1. Binding affinity ΔG (kcal/mol) for each tested MPs with DNA gyrase B version.

Microplastics	*F. nucleatum*	*D. longicatena*	*Coprococcus* sp
polycarbonate1	-7.7	-7.1	-7.5
Polycarbonate2	-5.7	-6.7	-5.6
Polycarbonate3	-8.8	-3.9	-10.2
Polyethylene terephthalate1	-6.2	-5.2	-5.7
Polyethylene terephthalate2	-5.1	-6.3	-6.6
Polyethylene terephthalate3	-7.4	-3.6	-7.2
polypropylene1	-4.6	-3.9	-4.3
Polypropylene2	-5.7	-5.1	-5.5
Polypropylene3	-6.0	-5.6	-5.5
polystyrene1	-5.2	-4.4	-4.9
Polystyrene2	-6.2	-5.3	-5.8
Polystyrene3	-8.5	-5.5	-7.2
polyethylene1	-2.9	-2.7	-2.7
Polyethylene2	-3.6	-3.2	-3.3
Polyethylene3	-4.0	-3.6	-4.1
polyurethane1	-4.8	-3.7	-4.3
Polyurethane2	-4.5	-4.1	-4.5
Polyurethane3	-5.3	-4.6	-4.6
polyvinylchloride1	-2.7	-2.4	-2.7
Polyvinylchloride2	-4.4	-3.8	-4.2
Polyvinylchloride3	-5.4	-4.7	-5.3

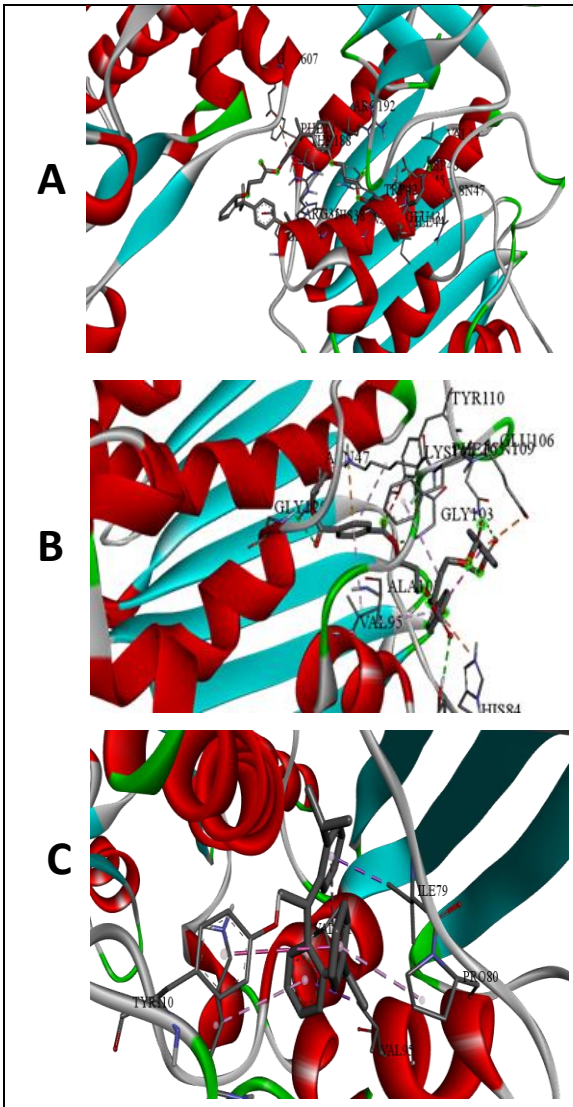

Fig.1: The optimal configuration of the polycarbonate3 (A), polyethylene terephthalate3 (B), and polystyrene3 (C) in the binding pocket of the 3D structure of DNA gyrase B of *F. nucleatum*

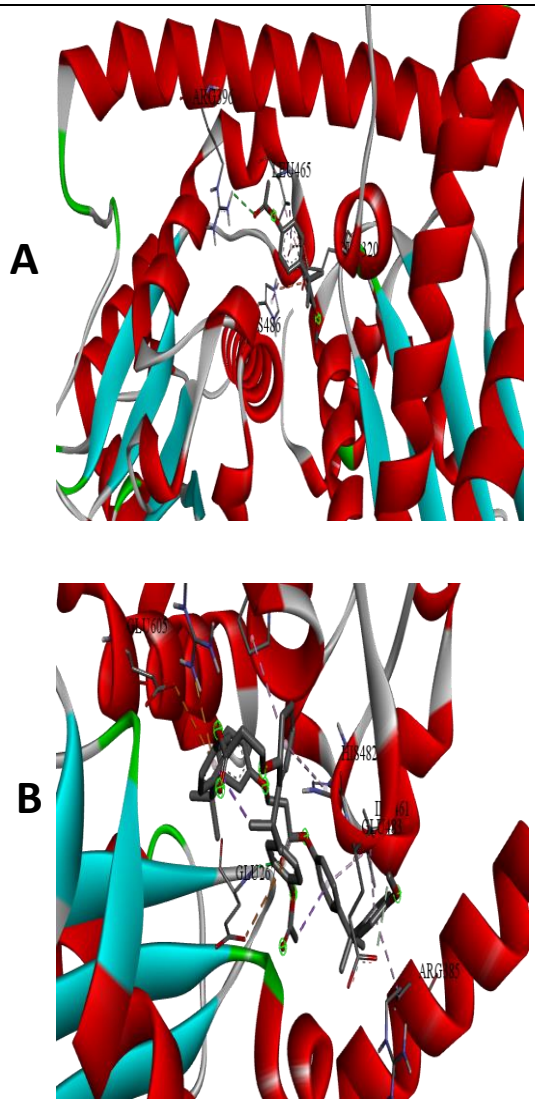

Fig.2: The optimal configuration of the polycarbonate1 **(A) ,** the polycarbonate3 (B), in the binding pocket of the 3D structure of DNA gyrase B of *D. longicatena.*

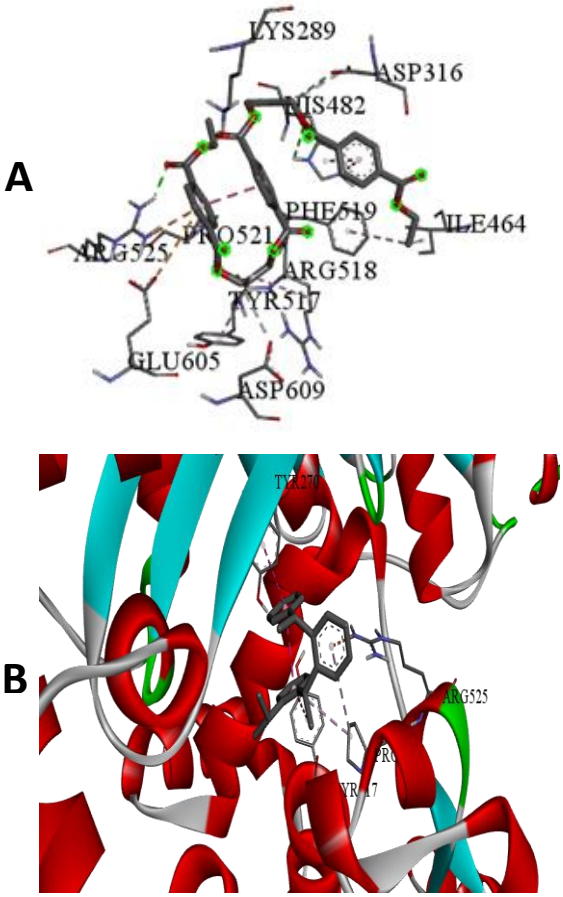

Fig. 3: The optimal configuration of the polyethylene terephthalate3 (A), polystyrene3 (B) in the binding pocket of the 3D structure of DNA gyrase B of *Coprococcus sp*.

The information in Table 2, provided insight into the interactions between polycarbonate3 (PC3) and the DNA gyrase B enzyme from *F. nucleatum*, which among the evaluated MPs for this organism had the highest binding affinity (-8.8 kcal/mol). In addition to forming a carbon-hydrogen bond with VAL45, PC3 also creates conventional hydrogen bonds with HIS38. Potential electrostatic attractions are suggested by the observation of pi-anion interactions between PC3 and the negatively charged side chains of ASP46 and GLU607. The overall binding affinity is also influenced by hydrophobic interactions, such as pi-sigma and pi-alkyl interactions.

Table 2. Interaction between PC3 and *F. nucleatum.*

Interaction	Distance	Category	Type
A:HIS38:HN - :UNL1:O	2.34129	Hydrogen Bond	Conventional Hydrogen Bond
A:HIS38:HD1 - :UNL1:O	1.27866	Hydrogen Bond	Conventional Hydrogen Bond
:UNL1:C - A:VAL45:O	2.55225	Hydrogen Bond	Carbon-Hydrogen Bond
A:ASP46:OD1 - :UNL1	3.55502	Electrostatic	Pi-Anion
A:GLU607:OE2 - :UNL1	4.38891	Electrostatic	Pi-Anion
A:THR188:CG2 - :UNL1	2.79895	Hydrophobic	Pi-Sigma
:UNL1 - A:VAL45	4.86074	Hydrophobic	Pi-Alkyl
:UNL1 - A:VAL41	4.4103	Hydrophobic	Pi-Alkyl
:UNL1 - A:VAL45	4.87363	Hydrophobic	Pi-Alkyl

Table 3, details the interactions between *F. nucleatum's* DNA gyrase B enzyme and polyethylene terephthalate3, with the latter showing a comparatively high binding affinity (-7.4 kcal/mol). Several typical hydrogen bonds are formed by polyethylene terephthalate3 with residues such as ASN47, TYR87, GLY103, ASN109, and GLY120, suggesting the possibility of stabilizing interactions. There are observed electrostatic interactions, including a pi-anion interaction with GLU106 and pi-cation interactions with HIS84 and LYS104. The total binding affinity is influenced by hydrophobic interactions, such as pi-alkyl interactions with PHE105, VAL95, LYS104, and ALA101.

The interactions between polystyrene3 and the *F. nucleatum* DNA gyrase B enzyme were shown in Table 4, where the enzyme showed a comparatively high binding affinity of -8.5 kcal/mol. The majority of contacts that polystyrene3 forms are hydrophobic these include pi-alkyl interactions with VAL121, LYS104, and PRO80, as well as pi-sigma interactions with ILE79 and VAL95. With TYR110, a pi-pi T-shaped interaction is seen, indicating possible aromatic stacking interactions. For polystyrene3, neither conventional hydrogen bonds nor electrostatic interactions are indicated, suggesting that hydrophobic forces dominate its binding.

Table 3. Interaction between polyethylene terephthalate3 with *F. nucleatum.*

Interaction	Distance	Category	Type
A:ASN47:HD22 - :UNL1:O	2.5447	Hydrogen Bond	Conventional Hydrogen Bond
A:TYR87:HH - :UNL1:O	2.76424	Hydrogen Bond	Conventional Hydrogen Bond
A:GLY103:HN - :UNL1:O	2.00921	Hydrogen Bond	Conventional Hydrogen Bond
A:ASN109:HD22 - :UNL1:O	2.67081	Hydrogen Bond	Conventional Hydrogen Bond
A:GLY120:HN - :UNL1:O	2.82686	Hydrogen Bond	Conventional Hydrogen Bond
A:HIS84:NE2 - :UNL1	3.98997	Electrostatic	Pi-Cation
A:LYS104:NZ - :UNL1	4.44616	Electrostatic	Pi-Cation
A:GLU106:OE2 - :UNL1	3.6247	Electrostatic	Pi-Anion
A:PHE105 - :UNL1	4.94672	Hydrophobic	Pi-Alkyl
:UNL1 - A:VAL95	4.79381	Hydrophobic	Pi-Alkyl
:UNL1 - A:LYS104	4.82111	Hydrophobic	Pi-Alkyl
:UNL1 - A:ALA101	4.77602	Hydrophobic	Pi-Alkyl

Table 4. Interaction between polystyrene3 with *F. nucleatum*.

Interaction	Distance	Category	Type
A:ILE79:CD1 - :UNL1	3.41396	Hydrophobic	Pi-Sigma
A:VAL95:CG1 - :UNL1	3.99954	Hydrophobic	Pi-Sigma
A:TYR110 - :UNL1	5.5726	Hydrophobic	Pi-Pi T-shaped
:UNL1 - A:VAL121	5.40376	Hydrophobic	Pi-Alkyl
:UNL1 - A:LYS104	5.16672	Hydrophobic	Pi-Alkyl
:UNL1 - A:PRO80	4.36037	Hydrophobic	Pi-Alkyl

The interactions between polycarbonate 1 (PC1) and the *D. longicatena* DNA gyrase B enzyme was displayed in Table 5. PC1 had a comparatively high binding affinity of -7.1 kcal/mol. PC1 and ARG396 establish a standard hydrogen bond. Pi-cation interactions with HIS486 and pi-anion interactions with GLU320 are two examples of the electrostatic interactions that are seen. The total binding affinity is influenced by hydrophobic interactions, such as a pi-sigma interaction with LEU465 and a pi-pi T-shaped interaction with HIS486.

The presence of pi-alkyl interactions with LEU465 enhances the hydrophobic contacts much more. The interactions between

polycarbonate3 (PC3) and the DNA gyrase B enzyme from *Coprococcus* sp. were detailed in Table 6. Of the evaluated MPs for this organism, PC3 had the highest binding affinity (-10.2 kcal/mol). PC3 combines with GLU267 to generate conventional hydrogen bonds and with GLU483 to form carbon-hydrogen bonds. Pi-cation/pi-donor hydrogen bond interactions with ARG525 and pi-anion interactions with GLU267 and GLU605 are among the electrostatic interactions that are seen. The overall binding affinity is influenced by hydrophobic interactions, which include pi-alkyl interactions with HIS482, ARG385, and ILE461, and alkyl interactions with PRO521 (Fig. 3).

Table 5. Interaction between PC1 with *D. longicatena.*

Interaction	Distance	Category	Type
A:ARG396:HH12 - :UNL1:O	2.93719	Hydrogen Bond	Conventional Hydrogen Bond
A:HIS486:NE2 - :UNL1	3.9255	Electrostatic	Pi-Cation
A:GLU320:OE2 - :UNL1	3.45633	Electrostatic	Pi-Anion
A:LEU465:CD1 - :UNL1	3.85323	Hydrophobic	Pi-Sigma
A:HIS486 - :UNL1	4.96031	Hydrophobic	Pi-Pi T-shaped
:UNL1 - A:LEU465	5.31505	Hydrophobic	Pi-Alkyl

Table 6. Interaction between PC3 and *Coprococcus* sp

Interaction	Distance	Category	Type
A:GLU267:HN - :UNL1:O	2.13624	Hydrogen Bond	Conventional Hydrogen Bond
:UNL1:C - A:GLU483:OE2	3.59381	Hydrogen Bond	Carbon-Hydrogen Bond
A:ARG525:NH2 - :UNL1	3.84633	Hydrogen Bond;Electrostatic	Pi-Cation;Pi-Donor Hydrogen Bond
A:GLU267:OE2 - :UNL1	4.37969	Electrostatic	Pi-Anion
A:GLU605:OE1 - :UNL1	4.8729	Electrostatic	Pi-Anion
A:PRO521 - :UNL1	4.97348	Hydrophobic	Alkyl
A:HIS482 - :UNL1	5.48443	Hydrophobic	Pi-Alkyl
:UNL1 - A:ARG385	4.38072	Hydrophobic	Pi-Alkyl
:UNL1 - A:ILE461	4.9116	Hydrophobic	Pi-Alkyl
:UNL1 - A:ILE461	4.04225	Hydrophobic	Pi-Alkyl

The interactions between DNA gyrase B from *Coprococcus* sp. and polyethylene terephthalate3 were shown in Table 7. The DNA gyrase B enzyme showed a comparatively high binding affinity (-7.2 kcal/mol). Several typical hydrogen bonds are formed by polyethylene terephthalate3 with residues such as LYS289, HIS482, and ARG525. ARG518 and ASP316 (two interactions) have many carbon-hydrogen bonds that are seen, which add to the binding affinity. Pi-cation interactions with HIS482 and ARG525 and a pi-anion contact with GLU605 are examples of electrostatic interactions. There are other hydrophobic interactions, like pi-pi stacking with HIS482, pi-alkyl interactions with TYR517 and PHE519, and alkyl interactions with ARG518 and ILE464. The DNA gyrase B enzyme from *Coprococcus* sp. displayed a particularly high binding affinity (-7.2 kcal/mol) in the interactions between polystyrene3.

ARG525 and polystyrene3 interact pi-cation, suggesting possible electrostatic attractions. The majority of contacts are hydrophobic; these include pi-alkyl interactions with PRO521 (two interactions) and pi-pi T-shaped interactions with TYR270 and TYR517. Polystyrene3 has no carbon-hydrogen nor typical hydrogen bonds specified, indicating that hydrophobic forces and electrostatic interactions dominate its binding.

Table 7. Interaction between polyethylene terephthalate3 with *Coprococcus* sp.

Interaction	Distance	Category	Type
A:LYS289:HZ1 - :UNL1:O	2.55384	Hydrogen Bond	Conventional Hydrogen Bond
A:HIS482:HD1 - :UNL1:O	2.81092	Hydrogen Bond	Conventional Hydrogen Bond
A:ARG525:HH12 - :UNL1:O	2.06609	Hydrogen Bond	Conventional Hydrogen Bond
:UNL1:C - A:ASP609:OD1	3.7885	Hydrogen Bond	Carbon-Hydrogen Bond
:UNL1:C - A:ARG518:O	3.63146	Hydrogen Bond	Carbon-Hydrogen Bond
:UNL1:C - A:ASP316:OD1	3.73303	Hydrogen Bond	Carbon-Hydrogen Bond
:UNL1:C - A:ASP316:OD2	3.68737	Hydrogen Bond	Carbon-Hydrogen Bond
A:HIS482:NE2 - :UNL1	3.8253	Electrostatic	Pi-Cation
A:ARG525:NH2 - :UNL1	3.87781	Hydrogen Bond;Electrostatic	Pi-Cation;Pi-Donor Hydrogen Bond
A:GLU605:OE1 - :UNL1	4.55869	Electrostatic	Pi-Anion
A:HIS482 - :UNL1	3.79587	Hydrophobic	Pi-Pi Stacked
A:ARG518 - :UNL1	5.38737	Hydrophobic	Alkyl
:UNL1:C - A:ILE464	5.29421	Hydrophobic	Alkyl
A:TYR517 - :UNL1	4.75713	Hydrophobic	Pi-Alkyl
A:PHE519 - :UNL1:C	4.98313	Hydrophobic	Pi-Alkyl

Table 8. Interaction between *Coprococcus* sp with polystyrene3.

Interaction	Distance	Category	Type
A:ARG525:NH2 - :UNL1	4.6504	Electrostatic	Pi-Cation
A:TYR270 - :UNL1	5.40708	Hydrophobic	Pi-Pi T-shaped
A:TYR517 - :UNL1	5.29463	Hydrophobic	Pi-Pi T-shaped
:UNL1 - A:PRO521	4.89614	Hydrophobic	Pi-Alkyl
:UNL1 - A:PRO521	5.33748	Hydrophobic	Pi-Alkyl

A thorough ADMET (Absorption, Distribution, Metabolism, Excretion, and Toxicity) analysis for polycarbonate MPs in various sizes (1bit, 2bit, and 3bit) was shown in Table (9) and Figure 4. When assessing a compound's pharmacokinetic behavior and possible toxicity in biological systems, ADMET qualities are essential.

Table 9. ADMET analysis for polycarbonate**.**

Compound	1bit	2bit	3bit
Pgp-inh	0.978	1	1
Pgp-sub	0.004	0.017	0.052
F(20%)	0.606	0.828	0.897
F(30%)	0.948	0.981	0.999
Caco-2	-4.991	-5.521	-5.915
MDCK	2.07E-05	1.19E-05	6.60E-06
BBB	0.272	0.024	0.003
PPB	96.70%	100.16%	105.50%
CYP1A2-inh	0.681	0.109	0.028
CYP1A2-sub	0.787	0.108	0.1
CYP2C19-inh	0.891	0.708	0.284
CYP2C19-sub	0.775	0.425	0.099
CYP2C9-inh	0.816	0.559	0.221
CYP2C9-sub	0.863	0.925	0.969

CYP2D6-inh	0.072	0.034	0
CYP2D6-sub	0.393	0.388	0.333
CYP3A4-inh	0.473	0.66	0.399
CYP3A4-sub	0.772	0.874	0.931
CL	2.91	1.229	2.285
hERG	0.068	0.514	0.303
DILI	0.578	0.545	0.589
Ames	0.009	0.074	0.066
Carcinogenicity	0.518	0.38	0.142
Respiratory	0.272	0.927	0.718
BCF	2.6	2.805	1.6
LC50DM	5.67	6.477	6.712
NR-AR	0.242	0.034	0.003
NR-AR-LBD	0.01	0.022	0.139
NR-AhR	0.016	0.023	0.03
NR-Aromatase	0.035	0.897	0.904
NR-ER	0.441	0.571	0.759
NR-ER-LBD	0.543	0.346	0.903
NR-PPAR-gamma	0.003	0.021	0.039
SR-ARE	0.371	0.868	0.868
SR-ATAD5	0.01	0.013	0.012
SR-HSE	0.029	0.388	0.429
SR-MMP	0.463	0.939	0.967
Flex	0.385	0.5	0.538
nStereo	0	1	1
NonBiodegradable	0	1	1
Skin_Sensitization	2	2	2

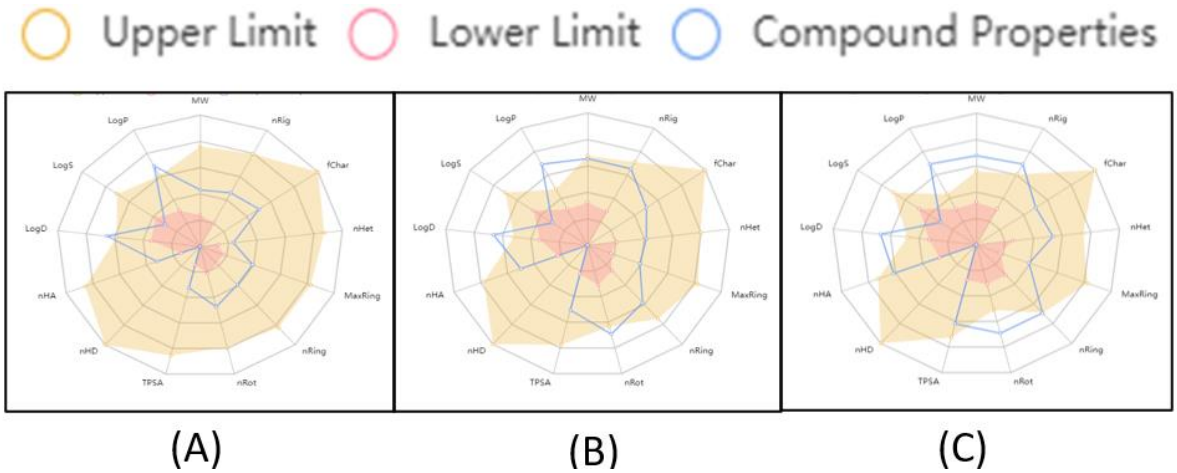

Fig. 4: The optimal and tested values of the polycarbonate1, 2 and 3 radar charts for ADMET (A), polycarbonate1 (B) polycarbonate2 (C) polycarbonate3, yellow region indicate to high level and maximum value opposite to red lines, while blue lines and regions for compound tested

DISCUSSION

For each of the examined MPs, the binding affinity ΔG (kcal/mol) with DNA gyrase B was demonstrated using three distinct organisms: *F. nucleatum*, *D. longicatena*, and *Coprococcus* sp. The MPs

and the enzyme have larger binding affinities when the ΔG values are lower, or more negatively correlated. Polycarbonate 3 has the highest binding affinity for all three organisms among the investigated MPs. This shows that polycarbonate3 may interact with DNA gyrase B very potently, possibly causing structural changes or disrupting the enzyme's ability to operate. By contrast, the lowest binding affinities are consistently displayed by polyethylene1, polyethylene2, and polyethylene3. These comparatively low binding affinities suggest that the DNA gyrase B enzyme and these MPs have a weaker interaction. It is interesting to note that different organisms can have varied binding affinities for the same MPs molecule. This variance in binding affinities raises the possibility that species-specific variations in the surroundings of binding sites or the architecture of the enzymes may have an impact on the interactions between MPs and enzymes (Jones *et al.,* 2008).

The present study examines the unique interactions between polycarbonate3 (PC3) and the DNA gyrase B enzyme from *F. nucleatum*. Of the MPs studied, PC3 demonstrated the highest binding affinity (-8.8 kcal/mol) for this organism. Listed interactions include a carbon-hydrogen bond with VAL45 and typical hydrogen bonds between PC3 and the HIS38 residue. The MPs-enzyme complex can be stabilized and the total binding affinity can be increased by these hydrogen bonding interactions. Furthermore, PC3 is found to interact pi-anionically with the negatively charged side chains of ASP46 and GLU607. By creating attractive forces, these electrostatic interactions may help direct the MPs toward the binding site and increase the binding affinity.

Additionally, there are hydrophobic interactions between PC3 and residues like THR188, VAL45, and VAL41, such as pi-sigma and pi-alkyl interactions. Through advantageous hydrophobic effects, these hydrophobic interactions can affect the MPs' location inside the binding site and potentially increase the total binding affinity (Chen *et al.,* 2021).

Through polar interactions, these hydrogen bonding interactions can improve the binding affinity and aid in the stability of the MPs-enzyme complex (Matta *et al.,* 2003). Additionally, electrostatic interactions are seen, such as a pi-anion contact with GLU106 and pi-cation interactions with HIS84 and LYS104. These electrostatic interactions can increase the binding affinity by creating attractive forces between the charged groups and the aromatic system of the MPs and help direct the MPs towards the binding site. The overall binding affinity is also influenced by hydrophobic interactions, such as pi-alkyl interactions with residues like ALA101, VAL95, LYS104, and PHE105. Through advantageous hydrophobic effects, these hydrophobic interactions can affect the orientation and placement of the MPs within the binding site.

The DNA gyrase B enzyme from *F. nucleatum* and polystyrene3 interacted with a comparatively high binding affinity of -8.5 kcal/mol. The majority of the interactions mentioned for polystyrene3 are hydrophobic. ILE79 and VAL95 exhibit pi-sigma interactions, whereas residues such as VAL121, LYS104, and PRO80 exhibit pi-alkyl interactions. Through advantageous hydrophobic effects, these hydrophobic interactions may affect the orientation and location of the MPs inside the binding site as well as the overall binding affinity. Furthermore, TYR110 exhibits a pi-pi T-shaped contact, indicating the possibility of aromatic stacking interactions between the MPs and the tyrosine residue's aromatic ring (Wheeler 2013). The binding affinity can be further enhanced by these pi-pi interactions by means of advantageous hydrophobic and dispersive forces. Interestingly, polystyrene3 has neither traditional hydrogen bonds nor electrostatic interactions described, suggesting that hydrophobic forces and aromatic stacking interactions are mainly responsible for polystyrene3's binding to the DNA gyrase B enzyme from *F. nucleatum*. Pi-cation interactions with HIS486 and pi-anion interactions with GLU320 are two

examples of the electrostatic interactions that are seen.

These interactions entail the attraction between the MPs' aromatic system and charged residues, which may direct the MPs in the direction of the binding site and increase the binding affinity. The overall binding affinity is also influenced by hydrophobic interactions. Possible aromatic stacking interactions are suggested by the observation of a pi-sigma interaction with LEU465, and a pi-pi T-shaped interaction with HIS486. Furthermore, pi-alkyl interactions with LEU465 improve the hydrophobic contacts between the enzyme and the MPs even more. The DNA gyrase B enzyme from *Coprococcus* sp., which demonstrated the highest binding affinity of -10.2 kcal/mol among the tested MPs for this organism, interacts with polycarbonate 3 (PC3), as table 6 illustrates. PC3 joins GLU267 in a normal hydrogen bond and GLU483 in a carbon-hydrogen bond. Through polar interactions, these hydrogen bonding interactions can improve the binding affinity and aid in stabilizing the MPs-enzyme complex (de Guzman *et al*., 2023). While PC3's aromatic components connect electrostatically with arginine (ARG525) and glutamic acid (GLU267, GLU605) residues, its carbonyl groups help form hydrogen bonds with glutamic acid residues (GLU267 and GLU483).

Hydrophobic contacts involving proline (PRO521), histidine (HIS482), arginine (ARG385), and isoleucine (ILE461) significantly enhance these interactions.

Pi-cation/pi-donor hydrogen bond interactions with ARG525 and pi-anion interactions with GLU267 and GLU605 are among the electrostatic interactions that are seen. The MPs may be guided towards the binding site by these electrostatic interactions, which also enhance the total binding affinity by creating an attractive force between the charged groups and the aromatic system of the MPs. Alkyl interactions with PRO521 and pi-alkyl contacts with HIS482, ARG385, and ILE461 are examples of hydrophobic interactions. Through advantageous hydrophobic effects, these hydrophobic interactions can affect the MPs' orientation and location inside the binding site (Atugoda *et al.,* 2021). PC3's strong binding affinity for the DNA gyrase B enzyme from *Coprococcus* sp. is probably due to the wide range of interactions it has been reported to exhibit with this organism, including hydrogen bonding, electrostatic interactions, and hydrophobic contacts. Additionally, the DNA gyrase B enzyme from *Coprococcus* sp. showed a remarkably high binding affinity of -7.2 kcal/mol in interactions with polyethylene terephthalate3. Several typical hydrogen bonds are formed by polyethylene terephthalate3 with residues such as LYS289, HIS482, and ARG525. The DNA gyrase B enzyme exhibited a noteworthy binding affinity of -7.2 kcal/mol with polyethylene terephthalate3 (PET3).

Multiple conventional hydrogen connections with lysine (LYS289), histidine (HIS482), and arginine (ARG525) residues are made possible by the ester groups in PET3's structure. The complex is additionally stabilized by carbon-hydrogen bonds with arginine (ARG518) and aspartic acid (ASP609, ASP316). The aromatic parts of PET3 participate in pi-anion interactions with glutamic acid (GLU605) and pi-cation interactions with histidine and arginine.

Protein-ligand complex stability and selectivity are known to be greatly enhanced by these hydrogen bonding interactions. Polyethylene terephthalate3 has been found to form several carbon-hydrogen bonds with residues such as ASP609, ARG518, and ASP316 (two interactions).

Although weaker than conventional hydrogen bonds, carbon-hydrogen bonds can still contribute favorable electrostatic interactions, which contribute to the overall binding affinity (Bissantz *et al.,* 2010). There are electrostatic interactions, a pi-anion interaction with GLU605 and a pi-cation interaction with HIS482 and ARG525. The delocalized electron systems of the MPs and the charged amino acid residues interact through attractive forces that can improve the binding affinity and specificity (Freire *et al.,*

2008). Alkyl interactions with ARG518 and ILE464, pi-alkyl interactions with TYR517 and PHE519, and hydrophobic interactions like pi-pi stacking with HIS482. Through advantageous desolvation effects and entropic benefits, hydrophobic interactions are recognized to be essential in promoting ligand association with protein binding sites and contributing to the overall binding affinity. Polyethylene terephthalate3 has demonstrated a wide variety of interactions with the DNA gyrase B enzyme from *Coprococcus* sp.

These interactions include hydrophobic contacts, electrostatic interactions, and hydrogen bonding. These interactions imply that the MPs may be able to form stable complexes with the enzyme, which may disrupt its function or cause conformational changes.

The DNA gyrase B enzyme from *Coprococcus* sp. showed a comparatively high binding affinity of -7.2 kcal/mol in its interactions with polystyrene3. Multiple conventional hydrogen connections with lysine (LYS289), histidine (HIS482), and arginine (ARG525) residues are made possible by the ester groups in PET3's structure. The complex is additionally stabilized by carbon-hydrogen bonds with arginine (ARG518) and aspartic acid (ASP609, ASP316).

The aromatic parts of PET3 are involvement in pi-anion interactions with glutamic acid (GLU605) and pi-cation interactions with histidine and arginine. One of the interactions mentioned for polystyrene3 is a pi-cation interaction with ARG525, which is related to the attraction between the MPs' delocalized electron system and positively charged arginine side chain. Through advantageous hydrophobic effects and dispersive forces, these hydrophobic interactions—especially the aromatic pi-pi and pi-alkyl interactions—can be extremely important in promoting the association of the MPs with the binding site.

Polystyrene3 (PS3) demonstrated a binding affinity that was similar to PET3 (-7.2 kcal/mol), but it had a different interaction profile. The majority of PS3's contacts are hydrophobic; these include pi-alkyl interactions with proline (PRO521) and pi-pi T-shaped interactions with tyrosine residues (TYR270 and TYR517). A cationic interaction with arginine (ARG525) complements these hydrophobic interactions. As MPs size increases, the absorption and solubility LogS (aqueous solubility) values decline and, for larger particles, fall below -5, indicating reduced solubility. The distribution coefficient (LogD) and partition coefficient (LogP) values rise with increasing size, which also shows that larger MPs have higher lipophilicity. The figure also shows that the limits of the blue lines are above the maximum value of the red regions. Particularly for bigger MPs, the F (20%) and F (30%) values—fractions of the substance absorbed at varying intestinal permeability levels—are comparatively high which, in the case of larger MPs, surpass 80% and show good absorption capacity based on ADMET-lab's calculations. Larger MPs may have reduced permeability (above -5.15, moderate), as indicated by the distribution and permeability Caco-2 and MDCK permeability values decreasing with increasing size

Conclusion

The results of our investigation demonstrate the intricate relationships that exist between MPs and the DNA gyrase B enzyme from different types of bacteria that are present in the human gut microbiome. Our models' binding affinities show that several MPs compounds—Polycarbonate3 in particular—have robust interactions with the DNA gyrase B enzyme in a variety of species, which may interfere with bacterial functioning. These interactions fuel the stability and specificity of the MPs-enzyme complexes by acting as a mix of hydrophobic effects, electrostatic forces, and hydrogen bonding. This study offers a fundamental understanding of the possible interactions between MPs and important bacterial enzymes in the human gut, which may cause microbial function alterations and negatively impact health outcomes. The findings

highlight the critical need for more investigation to clarify the mechanisms behind these interactions and evaluate the potential benefits of MPs in general for gut health.

Declarations:

Ethical Approval: Not applicable

Author Contributions: Conceptualization suggestion and project administration were done by Abdulmajeed Alqurashi, Ahmed G. Soliman and Sabry A. El-Naggar; methodology, software, formal analysis, investigation, resources, data curation, software and funding acquisition, validation, were carried out by Abdulmajeed Alqurashi, Ahmed G. Soliman and Sabry A. El-Naggar; original draft preparation, was written by Abdulmajeed Alqurashi, Ahmed G. Soliman and Sabry A. El-Naggar; writing—review, editing, and visualization were done by Abdulmajeed Alqurashi, supervision, was done by Abdulmajeed Alqurashi, Ahmed G. Soliman and Sabry A. El-Naggar

Conflict of interests: The authors declare no conflicts of interest.

Funding: This work did not receive any specific grant from funding agencies in the public, commercial, or not-for-profit sectors.

Availability of Data and Materials: All data used to conduct this study is provided within the manuscript and as supplementary material.

Acknowledgements: We would also like to thank Dr. Fisal al-rdadi and Dr. Ayman al-kariem.

REFERENCES

Anwaruzzaman, M., Haque, M. I., Sajol, M. N. I., Habib, M. L., Hasan, M. M., and Kamruzzaman, M. (2022). Micro and nanoplastic toxicity on aquatic life: fate, effect and remediation strategy. In *Biodegradation and Detoxification of Micropollutants in Industrial Wastewater* (pp. 145-176). Elsevier.

Atugoda, T., Vithanage, M., Wijesekara, H., Bolan, N., Sarmah, A. K., Bank, M. S., You, S., and Ok, Y. S. (2021). Interactions between microplastics, pharmaceuticals and personal care products: Implications for vector transport. *Environment International*, *149*, 106367.

Awuchi, C. G., and Awuchi, C. G. (2019). Impacts of plastic pollution on the sustainability of seafood value chain and human health. *International Journal of Advanced Academic Research*, *5*(11), 46-138.

Bajt, O. (2021). From plastics to microplastics and organisms. FEBS Open Bio, 11(4), 954-966.

Bhattacharya, A., and Khare, S. (2022). Ecological and toxicological manifestations of microplastics: current scenario, research gaps, and possible alleviation measures. *Journal of Environmental Science and Health, Part C*, *38*(1), 1-20.

Bissantz, C., Kuhn, B., and Stahl, M. (2010). A medicinal chemist's guide to molecular interactions. *Journal of medicinal chemistry*, *53*(14), 5061-5084.

Chen, X., Li, X., and Li, Y. (2021). Toxicity inhibition strategy of microplastics to aquatic organisms through molecular docking, molecular dynamics simulation and molecular modification. *Ecotoxicology and Environmental Safety*, *226*, 112870.

Cherinka, B., Andrews, B. H., Sánchez-Gallego, J., Brownstein, J., Argudo-Fernández, M., Blanton, M., Bundy, K., Jones, A., Masters, K., and Law, D. R. (2019). Marvin: A tool kit for streamlined access and visualization of the SDSS-IV MaNGA data set. *The Astronomical Journal*, *158*(2), 74.

de Guzman, M. K., Stanic-Vucinic, D., Gligorijevic, N., Wimmer, L., Gasparyan, M., Lujic, T., Vasovic, T., Dailey, L. A., Van Haute, S., & Velickovic, T. C. (2023). Small polystyrene microplastics interfere with the breakdown of milk proteins during static in vitro simulated human gastric digestion.

Environmental Pollution, 335, 122282.

Freire, E., Oddo, C., Frappier, L., and de Prat-Gay, G. (2008). Kinetically driven refolding of the hyperstable EBNA1 origin DNA-binding dimeric β-barrel domain into amyloid-like spherical oligomers. *Proteins: Structure, Function, and Bioinformatics*, *70*(2), 450-461.

Gomaa, E. Z. (2020). Human gut microbiota/microbiome in health and diseases: a review. *Antonie Van Leeuwenhoek*, *113*(12), 2019-2040.

Hanwell, M. D., Curtis, D. E., Lonie, D. C., Vandermeersch, T., Zurek, E., and Hutchison, G. R. (2012). Avogadro: an advanced semantic chemical editor, visualization, and analysis platform. *Journal of cheminformatics*, *4*, 1-17.

Jones, B. V., Begley, M., Hill, C., Gahan, C. G., and Marchesi, J. R. (2008). Functional and comparative metagenomic analysis of bile salt hydrolase activity in the human gut microbiome. *Proceedings of the National Academy of Sciences*, *105*(36), 13580-13585.

Liu, Y., Yang, X., Gan, J., Chen, S., Xiao, Z.-X., and Cao, Y. (2022). CB-Dock2: Improved protein–ligand blind docking by integrating cavity detection, docking and homologous template fitting. *Nucleic acids research*, *50*(W1), W159-W164.

Matta, C. F., Hernández-Trujillo, J., Tang, T. H., and Bader, R. F. (2003). Hydrogen–hydrogen bonding: a stabilizing interaction in molecules and crystals. *Chemistry–A European Journal*, *9*(9), 1940-1951.

Moeller, A. H., and Sanders, J. G. (2020). Roles of the gut microbiota in the adaptive evolution of mammalian species. *Philosophical Transactions of the Royal Society B*, *375*(1808), 20190597.

Morris, G. M., Huey, R., Lindstrom, W., Sanner, M. F., Belew, R. K., Goodsell, D. S., and Olson, A. J. (2009). AutoDock4 and AutoDockTools4: Automated docking with selective receptor flexibility. *Journal of computational chemistry*, *30*(16), 2785-2791.

Pirsaheb, M., Hossini, H., and Makhdoumi, P. (2020). Review of microplastic occurrence and toxicological effects in marine environment: Experimental evidence of inflammation. *Process Safety and Environmental Protection*, *142*, 1-14.

Tabl G, El-Naggar S, El-Desouki N, and Elmorsi H. (2023):'Long-term administrations of microplastics induces hepatorenal and intestinal tissues damages in experimental mice', *Biological and Biomedical Journal,* (2), 43-57.

Wheeler, S. E. (2013). Understanding substituent effects in noncovalent interactions involving aromatic rings. *Accounts of chemical research*, *46*(4), 1029-1038.

Xiong, G., Wu, Z., Yi, J., Fu, L., Yang, Z., Hsieh, C., Yin, M., Zeng, X., Wu, C., and Lu, A. (2021). ADMETlab 2.0: an integrated online platform for accurate and comprehensive predictions of ADMET properties. *Nucleic acids research*, *49*(W1), W5- W14